STM-Based Molecular Junction of Carbon Nano-Onion

Slawomir Sek,[c] Joanna Breczko,[a] Marta E. Plonska-Brzezinska,*[a] Agnieszka Z. Wilczewska,[a] and Luis Echegoyen*[b]

A significant amount of research has been done in the field of fullerenes since their discovery in 1985 by Smalley, Curl, and Kroto.[1] Fullerenes exhibit interesting properties, such as large surface areas, high thermal stability, and broad absorption spectra.[2,3] One of the most attractive and potentially useful properties of fullerenes is their ability to reversibly accept multiple electrons. For example, C_{60} and C_{70} are capable of forming hexa-anions in solution.[4] These remarkable electronic properties have been the basis for employing these molecules in the fabrication of photovoltaic cells, molecular electronics, and capacitors.[5,6] Since the discovery of carbon nanotubes (CNTs) by Iijima in 1991,[7] carbon nano-objects, such as nanotubes, nano-onions (CNOs), graphene, nanobuds, and peapods have received considerable attention. Carbon nanotubes are useful materials in a variety of applications, particularly in biosensing,[8] in designing novel therapeutic strategies,[9–12] field-effect transistors,[13] and as electrochemical capacitors.[14,15] Despite the fast progress, there are still numerous challenges related mainly to issues concerning reproducible separation of CNTs with well-defined structures and physico-chemical properties.

Although the discovery of CNOs by Ugarte[16] and Iijima[17,18] was almost concurrent with that of the CNTs, progress in this field has been very slow. Our current research has been centered mainly on carbon-based materials, such as CNOs, which represent a structural link between the fullerenes and the multi-wall carbon nanotubes. The CNO structures consist of a hollow spherical fullerene core surrounded by concentric and curved graphene layers with increasing diameters. The distance between the layers is very close to the interlayer distance in bulk graphite (0.34 nm).[19] CNOs have attracted considerable attention because of their unique physical and chemical properties. The thermogravimetric analysis of carbon nano-onions shows high thermal stability for these nanoparticles in air, even higher than for C_{60}.[20] Besides higher thermal stability, they also show higher chemical reactivity compared to CNTs. Another very interesting observation is that CNOs obtained from nano-diamonds are paramagnetic and have unpaired electrons on their surfaces, which has been confirmed by electron paramagnetic resonance.[20] The high temperature annealing of ultra-dispersed nano-diamonds (5 nm, average size) leads to their transformation into the CNO structure (5–6 nm in diameter, 6–8 shells).[21] CNOs have a variety of potential applications, including optical limiting,[22] field emission in solar cells,[23] fuel cell electrodes,[24] biosensors,[25] hyperlubricants,[26] and material and composite electrodes.[27,28]

Since the ability of CNOs to act as an electrically conductive medium is crucial for numerous applications, we analyzed the electronic conductance of single CNO structures. CNOs were functionalized with sulfide-terminated chains in order to trap molecules in metal–molecule–metal junctions. This approach involves the use of scanning tunneling microscopy (STM)-based molecular junctions, that is, entrapment of single molecules between a gold substrate and a gold STM tip.[29,30] As demonstrated by several groups, this method provides reproducible results for conductance measurements for n-alkanedithiols.[31–33] Moreover, it was successfully utilized for the studies of more complex systems, such as oligophenylethynylenes,[34] polyenes,[35] peptides,[36] and DNA.[37] Conductance measurements of functionalized C_{60} were also reported and redox-induced switching was demonstrated.[38]

The functionalization of CNO was performed using the amidation reaction with oxidized CNTs and 2-amino-1-ethane methyl disulfide (**1**) or 3-amino-1-propane methyl disulfide (**2**) as described in the Scheme 1. The molecule represented as CNO–$(CONH–(CH_2)_n–SH)_m$ was entrapped between two metallic contacts established by a gold substrate and a gold STM tip. The conductance measurements for sulfide-terminated CNOs were carried out using the STM-based molecular junction approach (see Scheme 2 for a representation of the general concept).

Figure 1a shows representative examples of the current–distance curves recorded for the single-molecule junction experiments using a bare gold substrate (-----) and a gold substrate covered with modified CNOs (——, ——, ——, and ——). These typical curves were recorded at a bias voltage of +0.5 V. The grey dashed curve displays a fast exponential decay of the current with increasing distance between the tip and the substrate. Such behavior is typical for electron tunneling between the tip and the bare gold surface. The current–distance curves recorded for the carbon material samples (solid curves) reveal different characteristics. Initially, the current decays with increasing distance between the tip and the substrate followed
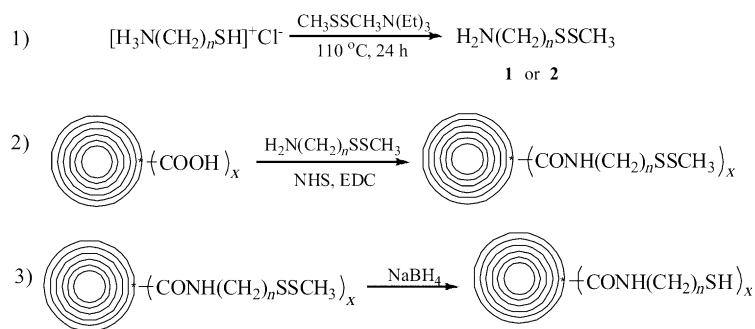
[a] J. Breczko,+ Dr. M. E. Plonska-Brzezinska,+ Dr. A. Z. Wilczewska
Institute of Chemistry
University of Bialystok
Hurtowa 1, 15-399 Bialystok (Poland)
E-mail: mplonska@uwb.edu.pl

[b] Prof. L. Echegoyen
Department of Chemistry
University of Texas at El Paso
500 W. University Ave., El Paso, TX 79968 (USA)
E-mail: echegoyen@utep.edu

[c] Dr. S. Sek+
Faculty of Chemistry
University of Warsaw
Pasteura 1, 02-093 Warsaw (Poland)

[+] These authors contributed equally to this work.

Supporting information for this article is available on the WWW under http://dx.doi.org/10.1002/cphc.201200624.

1)
$$[H_3N(CH_2)_nSH]^+Cl^- \xrightarrow[110\ ^\circ C,\ 24\ h]{CH_3SSCH_3N(Et)_3} H_2N(CH_2)_nSSCH_3$$
$$\mathbf{1}\ \text{or}\ \mathbf{2}$$

2)
$$(COOH)_x \xrightarrow[NHS,\ EDC]{H_2N(CH_2)_nSSCH_3} (CONH(CH_2)_nSSCH_3)_x$$

3)
$$(CONH(CH_2)_nSSCH_3)_x \xrightarrow{NaBH_4} (CONH(CH_2)_nSH)_x$$

Scheme 1. Functionalization of CNOs with thiol derivatives. **1**: $H_2N(CH_2)_2SSCH_3$; **2**: H_2N-$(CH_2)_3SSCH_3$; NHS: *N*-hydroxysuccinimide; EDC: *N*-(3-Dimethylaminopropyl)-*N'*-ethylcarbo-diimide hydrochloride.
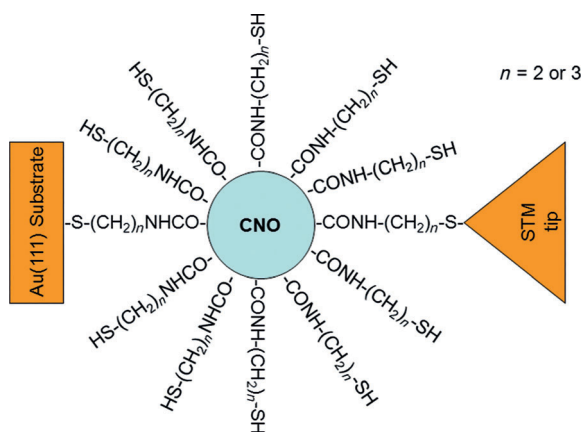

Scheme 2. STM-based molecular junction.
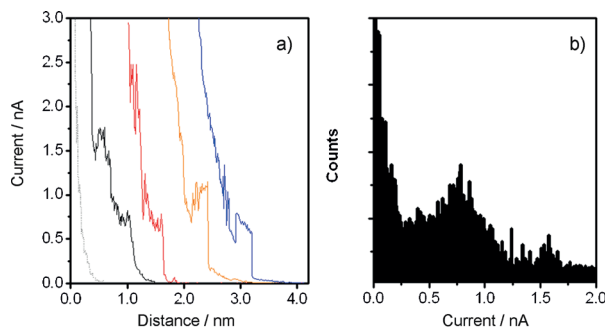
Figure 1. a) Current–distance curves recorded for bare sample (- - - -) and in the presence of CNO–(CONH–(CH₂)₂–SH)ₓ (——, ——, ——, and ——). b) Exemplary histograms constructed on the basis of current–distance curves (300 curves).

by a current step. The value of the current at the plateau is related to the conduction through the molecule (or molecules) trapped between the tip and the substrate.[29,30] The current remains constant as long as the molecule is bonded to the metallic contacts, but once the contact is broken the conductivity of the gap becomes very low, and the current drops suddenly. Figure 1b shows a representative histogram obtained from current–distance curves recorded for modified gold samples. The histograms display peaks corresponding to the value of the current which occurred most frequently for the current–

distance curves. In other words, the maximum is located at the value corresponding to the current plateaus and it corresponds to the conductance of the molecule trapped between the metallic contacts.

Based on the measurements performed at different bias voltages, we were able to obtain current–voltage characteristics for all of the systems studied. As can be seen in Figure 2, the *i–V* curves are symmetric and display a sigmoidal shape. By analyzing the linear part of the current–voltage plots, that is, at bias voltages between −0.4 and +0.4 V, we determined the conductance for each system.[39] The results are shown in Table 1.

The conductance values for the CNOs modified with (–CONH–(CH₂)₂–SH) chains are significantly
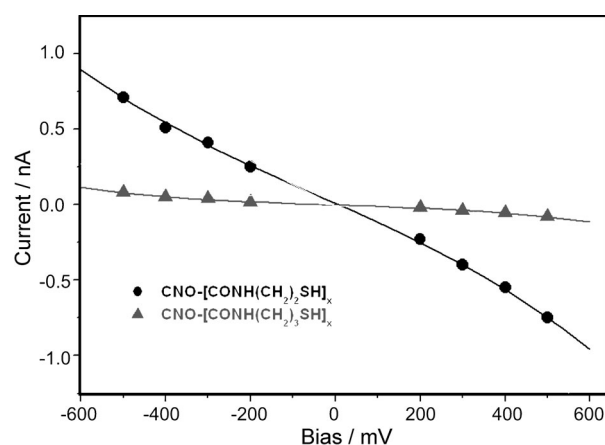
Figure 2. Current–voltage characteristics obtained on the basis of current–distance curves recorded at different bias voltages.

Table 1. Conductance of the junctions.

Sample	Conductance [nS]
CNO–(CONH–(CH₂)₂–SH)ₓ	1.4 ± 0.1
CNO–(CONH–(CH₂)₃–SH)ₓ	0.16 ± 0.05

higher than those obtained for the CNOs modified with longer chains (–CONH–(CH₂)₃–SH). This result was anticipated since the longer chains provide a higher barrier for tunneling and consequently the conductance is one order of magnitude lower.[31] This shows that the overall electron transmission through the CNOs is strongly affected by the presence of modifying chains, which determine the tunneling barrier. This is supported by the fact that the conductances measured for the systems studied here are comparable to those reported for n-alkanedithiols composed of eight to ten methylene groups.[31–33] If we consider the length of the chains involved in the electron transfer (excluding the core of the system, that is, the CNO), we conclude that the pathway is composed of either ten or twelve atoms for (–CONH–(CH₂)₂–SH) and (–CONH–(CH₂)₃–SH), respectively (Scheme 2).

In order to evaluate the efficiency of electron transmission through the junctions, we calculated the decay factors (β) for the CNO systems modified with ($-CONH-(CH_2)_2-SH$) and ($-CONH-(CH_2)_3-SH$). The determination of β was carried out using Equation (1):

$$\ln\frac{G_1}{G_2} = \beta(n_2 - n_1) \tag{1}$$

where G_1 is the conductance obtained for molecules modified with ($-CONH-(CH_2)_2-SH$), G_2 is the conductance obtained for molecules modified with ($-CONH-(CH_2)_3-SH$), n_1 is the number of backbone atoms within ($-CONH-(CH_2)_2-SH$) separating the metallic contacts of the junction, that is, $n_1 = 10$, and n_2 is the number of backbone atoms within ($-CONH-(CH_2)_3-SH$), that is, $n_2 = 12$. The decay factors were $\beta = 1.08$ per atom for the modified CNOs. The magnitude of the decrease in conductance expressed as decay factor β is important, if we consider the detailed mechanism of electron transfer through the molecules of interest. The values obtained in this work confirm that electron transmission through the junctions occurs by a superexchange mechanism, as they are similar to those observed for electron tunneling through alkyl bridges, which usually range between $\beta = 0.8$ and 1.2 per atom.[31–33] Comparison of the conductances determined for CNO-thiol derivatives in our laboratory and for C_{60} having an amino-terminated linker[39] with chains of the same length show that the electron transport is more efficient for the C_{60} system (Scheme 3).
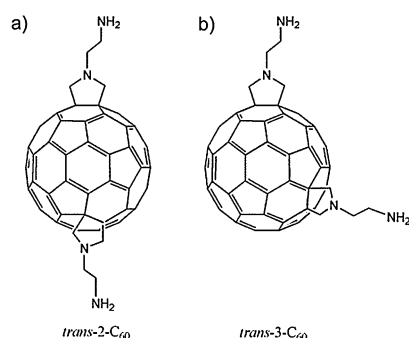
Scheme 3. Chemical structures of *trans*-2-C_{60} and *trans*-3-C_{60}.[38]

Gaussian curve fitting resulted in a single-molecule conductance of 4.9 ± 1.7 nS for *trans*-2-C_{60} and 7.9 ± 2.8 nS for *trans*-3-C_{60} in DMF (Scheme 3).[38] There are several factors which can be considered as origin for the observed difference. First, the conductance measurements for *trans*-2-C_{60} or *trans*-3-C_{60} were performed in a liquid environment. The presence of the solvent as well as electrolyte ions may change the charge distribution relative to air. Another issue is related to the extent of the core modification. In our case the CNO core experiences an extensive modification of the surface, the *trans* derivatives of C_{60}, however, possess only two groups. In other words, the latter has a much better defined geometry of the junction and as a consequence a better defined through-bond electron-transfer pathway. On the other hand, the multiple chains on

the CNO core may give rise to interchain electron hopping or electron tunneling through van der Waals bridges, which is less effective compared to an exclusive through-bond mechanism.[40] Finally, the difference in conductance may also result from the nature of the core, that is, C_{60} may provide a more efficient medium for electron transfer compared to the CNO core. In order to check this assumption, we estimated the values of the conductances for unmodified CNOs by extrapolating the conductance values to $n = 0$ and obtained a value of ~ 71.8 µS for CNOs. The conductance values reported in the literature for a pristine C_{60} cover quite a broad range. For example, measurements based on mechanically controlled break junctions (MCBJ) indicate that the conductance of unmodified C_{60} trapped between two gold electrodes is 7.75 µS.[41] STM-based measurements utilizing current–distance spectroscopy on C_{60} deposited on a copper surface resulted in a value of 20 µS.[42] Both values are lower than the extrapolated conductance estimated for a bare CNO. The latter is much closer to metallic behavior.[43] However, the extrapolated value should be considered with care since the above mentioned tunneling through the van der Waals bridges may contribute to a higher decay constant.[40] It must be emphasized that the approaches utilized for the C_{60} conductance measurements involve physical contact between the electrodes and the molecule with no intermediate chemical linker. This may lead to mechanical deformation of the entrapped species resulting in a change of the charge distribution and its electron-transfer mediating properties.[44] Thus, we can only conclude that the intrinsic conductances of CNOs and C_{60} are within the same order of magnitude. This result was somewhat surprising but very promising within the context of potential applications of CNOs in molecular electronics.

Experimental Section

Formation of Junctions and Conductance Measurements

In all experiments we used gold substrates (Arrandee) with 200–300 nm thick gold films evaporated on borosilicate glass slides pre-coated with 1–4 nm adhesive layers of chromium. Prior to each experiment the substrates were carefully flame-annealed to form atomically flat Au (111) terraces. The monolayers of modified CNO were prepared by a self-assembly method from ethanol solutions. The substrates were soaked for 24 h. After the deposition, the samples were rinsed with ethanol and water. Molecular junctions were formed using dry samples.

Conductance measurements were carried out using Agilent 5500AFM (Agilent Technologies, Santa Clara, CA, USA). All data were taken under ambient conditions in air. For the molecular junction experiments we used gold tips prepared by cutting a 0.25 mm gold wire (99.99%, Aldrich). The junctions were formed using the STM-based method.[29,30,32] The gold STM tip was placed at a chosen location on the sample surface and the tunneling-current setting determined the initial distance between the tip and the substrate. The values of the initial current were always sufficiently high to provide the contact between the tip and the molecules adsorbed on the gold surface. At these conditions it is expected that gold tip interacts with the terminal thiol groups of the modified CNO and Au–S bonds are formed. Further, the feedback

system was disabled and the tip was elevated while keeping constant x-y positions. During the vertical movement of the tip, the current was recorded as a function of the tip–sample distance. This procedure was repeated several hundred times for each sample in order to obtain reliable statistics. At least 300 curves measured on five independent samples were used to construct the histograms for each type of monolayer. The conductance of the junctions was measured within the bias voltage range from −0.5 V to +0.5 V.

Synthesis of 2-Amino-1-Ethane Methyl Disulfide (1) and 3-Amino-1-Propane Methyl Disulfide (2)

The mixture of 0.4 g (5 mmol) of cysteamine hydrochloride or 3-amino-1-propanethiol, 2 mL of dimethyl disulfide, and 0.1 mL of triethylamine was heated at 110 °C for 24 h. The unreacted dimethyl disulfide was evaporated under reduced pressure. Toluene was added to the crude product to remove unreacted residues by azeotropic distillation.

1: 1H NMR (MHz, CD_3OD): $\delta = 2.31$ (s, CH_3), 2.79 (t, CH_2), 2.92 ppm (t, CH_2). FT-IR: $\tilde{v} = 3332$ (v_{NH}), 2917 (v_{CH2}), 2849 (v_{CH2}), 1659 (v_{NH2}), 1433 cm^{-1} (δ_{CH2}).
2: 1H NMR (MHz, CD_3OD): $\delta = 1.86$ (m, CH_2), 2.35 (s, CH_3), 2.59 (t, CH_2), 2.72 ppm (t, 2 H, CH_2). FT-IR: $\tilde{v} = 3335$ (v_{NH}), 2922 (v_{CH2}), 2853 (v_{CH2}), 1568 (v_{NH2}), 1401 cm^{-1} (δ_{CH2}).

Synthesis of Sulfide-Terminated CNOs

The non-modified CNOs were obtained by annealing nano-diamonds of 5 nm average particle size under a positive pressure of helium at 1650 °C.[45] The functionalization of CNOs was conducted as originally described by Lieber et al. for single-walled nanotubes,[46] and later adapted to the CNOs in our laboratory.[20] High resolution transmission electron microscopy images of the CNOs were reported elsewhere.[20] 20 mg of crude 6–8 shell CNOs were dispersed by ultrasonication for 30 min and refluxed for 48 h (CNOs) in 3.0 M aqueous nitric acid. The mixture was then centrifuged for 10 min and the black powder collected in the bottom of the test tube was washed several times with 0.1 M NaOH, deionized water and dried overnight in a vacuum oven (T = 120 °C), to yield ox-CNOs. A 100 µL of ox-CNOs solution (5 mg mL^{-1}), activated by 50 µL N-(3-Dimethylaminopropyl)-N′-ethylcarbodiimide hydrochloride (EDC, 100 mg mL^{-1}) and 50 µL N-hydroxysuccinimide (NHS, 50 mg mL^{-1}), was added to 10 mL of HEPES (1 M 4-(2-hydroxyethyl)piperazine-1-ethanesulfonic acid in H2O buffer, pH 7.2). Next, disulfide **1** or **2** was added to the solution, and the amidation reaction with ox-CNOs were performed (Scheme 1). The reduction reaction with NaBH4 was conducted to CNO–(CONH–(CH)$_n$–SH)$_m$ (n = 2 or 3).

Acknowledgements

[1] H. W. Kroto, J. R. Heath, S. C. Obrien, R. F. Curl, R. E. Smalley, *Nature* **1985**, *318*, 162–163.
[2] V. I. Borodin, V. A. Trukhacheva, *Tech. Phys. Lett.* **2004**, *30*, 598–599.
[3] K. Harigaya, S. Abe, *Phys. Rev. B* **1994**, *49*, 16746–16752.
[4] Q. Xie, E. Perez-Cordero, L. Echegoyen, *J. Am. Chem. Soc.* **1992**, *114*, 3978–3980.
[5] P. Jarillo-Herrero, J. Kong, H. S. J. van der Zant, C. Dekker, L. P. Kouwenhoven, S. De Franceschi, *Nature* **2005**, *434*, 484–485.
[6] N. Martín, *Chem. Commun.* **2006**, *20*, 2093–2104.
[7] S. Iijima, *Nature* **1991**, *354*, 56–58.
[8] J. Wang, *Electroanalysis* **2005**, *17*, 7–14.
[9] F. Karchemski, D. Zucker, Y. Barenholz, O. Regev, *J. Controlled Release* **2012**, *160*, 339–345.
[10] A. Bianco, K. Kostarelos, M. Prato, *Curr. Opin. Chem. Biol.* **2005**, *9*, 674–679.
[11] S. K. Smart, A. I. Cassady, G. Q. Lu, D. J. Martin, *Carbon* **2006**, *44*, 1034–1047.
[12] X. Zhang, Z. Hui, D. Wan, H. Huang, J. Huang, H. Yuan, J. Yu, *Int. J. Biol. Macromolecules* **2010**, *47*, 389–395.
[13] R. Martel, T. Schmidt, H. R. Shea, T. Hertel, Ph. Avouris, *Appl. Phys. Lett.* **1998**, *73*, 2447–2449.
[14] Ch. Du, N. Pan, *Nanotechnology* **2006**, *17*, 5314–5318.
[15] H. Pan, J. Li, Y. P. Feng, *Nanoscale Res. Lett.* **2010**, *5*, 654–668.
[16] D. Ugarte, *Nature* **1992**, *359*, 707–709.
[17] S. Iijima, *J. Cryst. Growth* **1980**, *50*, 675–683.
[18] S. Iijima, *J. Phys. Chem.* **1987**, *91*, 3466–3467.
[19] H. Hiura, T. W. Ebbesen, J. Fujita, K. Tanigaki, T. Takada, *Nature* **1994**, *367*, 148–151.
[20] A. Palkar, F. Melin, C. M. Cardona, B. Elliott, A. K. Naskar, D. D. Edie, A. Kumbhar, L. Echegoyen, *Chem. Asian J.* **2007**, *2*, 625–633.
[21] V. L. Kuznetsov, A. L. Chuvilin, Y. V. Butenko, I. Y. Malkov, V. M. Titov, *Chem. Phys. Lett.* **1994**, *222*, 343–348.
[22] E. Koudoumas, O. Kokkinaki, M. Konstantaki, S. Couris, S. Korovins, P. Detkov, V. Kuznetsov, S. Pimenov, V. Pustovoi, *Chem. Phys. Lett.* **2002**, *357*, 336–340.
[23] M. Choi, I. S. Altman, Y. J. Kim, P. V. Pikhitsa, S. Lee, G. S. Park, T. Jeong, J. B. Yoo, *Adv. Mater.* **2004**, *16*, 1721–1725.
[24] H. Wang, T. Abe, S. Maruyama, Y. Iriyama, Z. Ogumi, Z. Yoshikawa, *Adv. Mater.* **2005**, *17*, 2857–2860.
[25] J. Luszczyn, M. E. Plonska-Brzezinska, A. Palkar, A. T. Dubis, A. Simionescu, D. T. Simionescu, B. Kalska-Szostko, K. Winkler, L. Echegoyen, *Chem. Eur. J.* **2010**, *16*, 4870–4880.
[26] Y. Liu, R. L. Vander Wal, V. N. Khabashesku, *Chem. Mater.* **2007**, *19*, 778–786.
[27] M. E. Plonska-Brzezinska, A. Palkar, K. Winkler, L. Echegoyen, *Electrochem. Solid-State Lett.* **2010**, *13*, K35–K38.
[28] J. Breczko, K. Winkler, M. E. Plonska-Brzezinska, A. Villalta-Cerdas, L. Echegoyen, *J. Mater. Chem.* **2010**, *20*, 7761–7768.
[29] B. Xu, N. J. Tao, *Science* **2003**, *301*, 1221–1223.
[30] W. Haiss, H. van Zalinge, S. J. Higgins, D. Bethell, H. Hobenreich, D. J. Schiffrin, R. J. Nichols, *J. Am. Chem. Soc.* **2003**, *125*, 15294–15295.
[31] X. Li, J. He, J. Hihath, B. Xu, S. M. Lindsay, N. J. Tao, *J. Am. Chem. Soc.* **2006**, *128*, 2135–2141.
[32] S. Sek, A. Misicka, K. Swiatek, E. Maicka, *J. Phys. Chem. B* **2006**, *110*, 19671–19677.
[33] W. Haiss, S. Martin, E. Leary, H. van Zalinge, S. J. Higgins, L. Bouffier, R. J. Nichols, *J. Phys. Chem. C* **2009**, *113*, 5823–5833.
[34] S. Martín, I. Grace, M. R. Bryce, C. Wang, R. Jitchati, A. S. Batsanov, S. J. Higgins, C. J. Lambert, R. J. Nichols, *J. Am. Chem. Soc.* **2010**, *132*, 9157–9164.
[35] J. He, F. Chen, J. Li, O. F. Sankey, Y. Terazono, C. Herrero, D. Gust, T. A. Moore, A. L. Moore, S. M. Lindsay, *J. Am. Chem. Soc.* **2005**, *127*, 1384–1385.
[36] S. Sek, K. Swiatek, A. Misicka, *J. Phys. Chem. B* **2005**, *109*, 23121–23124.
[37] E. Wierzbinski, J. Arndt, W. Hammond, K. Slowinski, *Langmuir* **2006**, *22*, 2426–2429.
[38] T. Morita, S. M. Lindsay, *J. Phys. Chem. B* **2008**, *112*, 10563–10572.
[39] D. J. Wold, C. D. Frisbie, *J. Am. Chem. Soc.* **2001**, *123*, 5549–5556.
[40] K. Slowinski, R. V. Chamberlain, C. J. Miller, M. Majda, *J. Am. Chem. Soc.* **1997**, *119*, 11910–11919.
[41] T. Bohler, A. Edtbauer, E. Scheer, *Phys. Rev. B* **2007**, *76*, 125432–125437.

[42] N. Néel, J. Kröger, L. Limot, T. Frederiksen, M. Brandbyge, R. Berndt, *Phys. Rev. Lett.* **2007**, *98*, 065502–065510.

[43] R. Landauer, *IBM J. Res. Dev.* **1957**, *1*, 223–231.

[44] C. Joachim, J. K. Gimzewski, H. Tang, *Phys. Rev. Lett.* **1998**, *58*, 16407–16417.

[45] A. S. Rettenbacher, B. Elliott, J. S. Hudson, A. Amirkhanian, L. Echegoyen, *Chem. Eur. J.* **2006**, *12*, 376–387.

[46] S. Wong, A. Woolley, E. Joselevich, C. Cheung, C. Lieber, *J. Am. Chem. Soc.* **1998**, *120*, 8557–8558.